Sinking Deltas

James P.M. Syvitski[1], Albert J. Kettner[1], Irina Overeem[1], Eric W.H. Hutton[1], Mark T. Hannon[1], G. Robert Brakenridge[2], John Day[3], Charles Vörösmarty[4], Yoshiki Saito[5], Liviu Giosan[6], Robert J. Nicholls[7]

[1]CSDMS Integration Facility, INSTAAR, University of Colorado, Boulder CO, 80309-0545
[2]Dartmouth Flood Observatory, Dartmouth College, Hanover, NH 03755
[3]Dept. of Oceanography and Coastal Sciences, Louisiana State University, Baton Rouge, LA 70803
[4]Dept. of Civil Engineering, City College of New York, City University of New York, NY 10035
[5]Geological Survey of Japan, AIST, Tsukuba 305-8567, Japan
[6]Woods Hole Oceanographic Institution, Woods Hole, MA 02543
[7]School of Civil Engineering and the Environment and Tyndall Centre for Climate Change Research, University of Southampton, SO17 IBJ UK

Abstract

The world's population living on low-lying deltas is increasingly vulnerable to flooding, whether from intense rainfall, rivers or from hurricane-induced storm surges. High-resolution SRTM and MODIS satellite data along with geo-referenced historical map analysis allows quantification of the extent of low-lying delta areas and the role of humans in contributing to their vulnerability. Thirty-three major deltas collectively include ~26,000 km^2 of area below local mean sea level and ~96,000 km^2 of vulnerable area below 2 m a.s.l. The vulnerable areas may increase by 50% under projected 21st Century eustatic sea level rise, a conservative estimate given the current trends in the reduction in sedimentary deposits forming on the surface of these deltas. Analysis of river sediment load and delta topographical data show that these densely populated, intensively farmed landforms, that often host key economic structures, have been destabilized by human-induced accelerated sediment compaction from water, oil and gas mining, by reduction of incoming sediment from upstream dams and reservoirs, and from floodplain engineering.

Introduction

Close to 0.5 billion people live on, or near, world deltas, inclusively in many mega-cities (1, 2). Ten countries (China, India, Bangladesh, Vietnam, Indonesia, Japan, Egypt, USA, Thailand, and the Philippines) account for 73% of the people that live in the world's coastal zone, defined as within 10 m a.s.l. (3). 20th-century catchment developments and population and economic growth within subsiding deltas have placed these environments and their populations under a growing risk of coastal flooding, wetland loss, shoreline retreat, and loss of infrastructure (4, 5). It is estimated that more than 10 million people per year experience flooding due to storm surges, and most of these people are living on Asian deltas (6). Using new, globally-consistent and high-resolution topographic data, three hypotheses are tested: 1) deltas are rapidly sinking, often to below local sea level, 2) the lack of sediment getting to delta floodplains is the main reason so many deltas are sinking, and 3) human activities are largely responsible for the present vulnerability of deltas. For a representative suite of deltas, Shuttle Radar Topography Mission (SRTM) data are applied to evaluate delta topography, in relation to mean sea level. Historical maps are geo-referenced against detailed topographic data to map morphodynamic patterns and quantify how rivers once flowed through deltas. Visible and near-infrared Moderate Resolution Imaging Spectroradiometer (MODIS) satellite images are used to assess flooding in modern deltas and investigate whether such flooding is mainly from river runoff or instead from coastal storm surges, and whether present river suspended load is sufficient to maintain delta plain aggradation and stability.

Background

Change in the position of a delta's surface relative to local mean sea level (Δ_{RSL}) is from the contribution of three components:

1) Changes to the volume of the global ocean (*Eustasy, E*) over time, as influenced by fluctuations in the storage of terrestrial water (e.g. glaciers, ice sheets, groundwater, lakes, and reservoirs), and fluctuations in temperature of the ocean's surface waters (7). Today E contributes ≈1.8 to 3 mm/y to Δ_{RSL} *(7, 8)* largely under the anthropogenic influence of global warming. The IPCC projected that sea level will likely rise by 21-71 cm by the year 2070 with a best estimate of 44 cm (7) but there is ongoing discussion on the dynamic response of the major ice sheets that could potentially contribute even more water over this period.

2) Vertical movements of the land surface (M), as influenced by hydro-isostasy related to sea level fluctuation, loading due to the weight of delta deposits, glacio-isostasy related to the growth or shrinkage of nearby ice masses (9), tectonics, and deep-seated thermal subsidence (5, 10, 11, 12). Tectonic subsidence along faults in the Mississippi delta contributes 5±2 mm/y to its Δ_{RSL} (13). The Earth's crust takes thousands of years to relax from loading changes (14) and displacements extend over a region much larger than the direct area of the load change. The six sediment lobes of the Holocene Mississippi delta, each weigh between 135 and 847 billion metric tons, and contribute up to 5 mm/y to its Δ_{RSL} (5, 15). While important, seldom are M contributions to a delta's Δ_{RSL} calculated, particularly with all its varied terms.

3) Changes to the sedimentary volume of delta deposits through *Natural Compaction* (C_n), *Accelerated Compaction* (C_A), and *Aggradation* (A). C_n involves natural changes in the void space within delta sediment (e.g. due to dewatering of soils and prodelta mud, grain-packing realignment, and natural organic matter oxidation) (16, 17). C_n typically contributes ≤3 mm/y to Δ_{RSL} (5). C_A is the anthropogenic contribution to this volume change, from subsurface mining of oil, gas or groundwater, soil drainage and oxidation. The effects may be localized but can be dramatic, e.g.: i) Yangtze: C_A =28 mm/y before controls on groundwater withdrawal came into effect circa 1965 (18), ii) Mississippi near New Orleans: C_A =5 to 25 mm/y (19), when organic soils are drained and oxidized (20), and gas is mined (21), iii) Niger: C_A =25 to 125 mm/y from petroleum mining (22), iv) Chao Phraya: C_A =50 to 150 mm/y from groundwater withdrawal (23), and v) Po: C_A =60 mm/y during the peak of methane mining (24). The Po Delta has subsided 3.7 m in the 20th Century, of which 81% is attributed to methane mining. After the cessation of methane extraction, the rate slowed to <25 mm/y by 1970 (25), and by the 1990's the subsidence rate was ≤4 mm/y (26).

Sediment input to deltas is highly dynamic and occurs as a hierarchy of pulses over a wide range of temporal and spatial scales (27). *Aggradation* (A) is the addition of volume from sediment that is delivered to and retained on the subaerial delta as new sedimentary layers. A has rates varying from 1-50 mm/y (Table 1). Flooding occurs from river overbanking, or local surface runoff related to intense rainfall, or from coastal storm surges. Most river floods bring high amounts of suspended load to a delta's surface, although upstream dam interception of river-borne sediment may leave a river with relatively clean river water, flowing with reduced flood magnitudes. Flooding from the ocean may contribute turbid water from tide or wave resuspension. For example, hurricane-generated storm surges add sediment to the outer portions of the Mississippi Delta (28, 29), whereas artificial levees confine the Mississippi River and prohibit river flooding on its delta plain.

Humans have often reduced the number of naturally occurring distributary channels, fixed their

location to support low-flow navigation, and protected populated areas from flooding by levees (1). *Aggradation* may thus be limited to within the distributary channels. On the Po Delta, artificial levees do not allow for upstream flood waves to overbank and penetrate the delta plain, consequently within-channel aggradation ranges from 20 to >60 mm/y (30). Levees will eventually cause super-elevation of the riverbed above the surrounding floodplain. If the distributary channels are free to migrate across the delta plain, or episodically switch their position, then the delta surface builds up as a series of fluvial deposits. In China, controlled flooding has even been used to raise land via sedimentation in the Yellow River Delta (31).

Sediment input to deltas has been reduced or eliminated at all scales (27). Delivery is often through distributary channels engineered to bypass and not interact with the delta plain (Table 1). The consequence is much reduced levels of delta plain aggradation. Lack of appreciation of the broad range of scales over which deltaic processes operate may lead to erroneous conclusions about how deltas function (32, 29, 17).

Often field measurements do not separate M, C_n, C_A and A as unique contributions to a delta's overall *Subsidence (S)* (relative sinking of the land surface). Large deltas have areas on the order of 10^4 to $>10^5$ km^2 and consequently S is spatially variable, depending on a location's unique load and compaction history. Seldom is an area-integrated S calculated. In one rare study, involving the Mississippi Delta, three independent data sources (Synthetic Aperture Radar, GPS geodesy, and leveling) identified an area-averaged S of 5 to 6 mm/y. This survey included parts of New Orleans that have subsided 25 mm/y over the last 150 years when major drainage and levee construction began after 1850 (19).

Methodology

Thirty-three representative deltas (Supplementary Figure 1) were examined using SRTM altimetry (see Table 1, Figs. 1-4). The altimetry has a vertical root mean square error between 1.1 to 1.6 m in lowland areas (15, 33). The horizontal footprint of a SRTM pixel is either 1-arc or 3-arc seconds. Deltas were examined for the extent and location of areas near or below sea level (<0 m and <2 m a.s.l.). We used the high-end sea level rise estimates (> 0.7-1.1 m) of suites of climate model scenarios (7) to estimate increases in vulnerable delta lowlands (< 3m a.s.l). MODIS imagery at between 250 and 500m resolution was used to map floodwater extent on deltas and indicate whether the water was rich in suspended sediment (Fig. 3, Table1, Supplementary Figures 3-8). Eighty-six historical maps (published between 1760 and 1922) of the selected deltas were analyzed for the location and number of distributary channels (Fig. 4, Table 1, Supplementary Figure 10).

Early-20th Century *Aggradation* rates (Table 1) are determined from a database of gauged river sediment loads that once reached the deltas, as measured before the proliferation of upstream dams (30, 34, 35, 23) and modeling of sediment retention on a delta per unit area (1). Small and steep gradient rivers retain little sediment as they cross their delta plain; retention rates are in the 10 to 20% range. Larger deltas with numerous distributary channels have a larger retention rate of 50 to 60%. 21st Century *Aggradation* rates (Table 1) use the previous estimates and adjust for Late 20th Century sediment reduction due to reservoir trapping and engineering control on river flooding. Most deltas saw their incoming sediment loads substantially reduced during the Late 20th Century, half by more than 50% (Table 1).

Subsidence values (Table 1) are from literature sources (e.g. 23, 36) and the Permanent Service for Mean Sea Level (PSMSL), hosted at the Proudman Oceanographic Laboratory (POL) (15). A word of caution on *Subsidence* rates: rates in the literature often are maximum rates within a delta, and not area integrated, whereas our calculated *Aggradation* rates are area-integrated rates.

Subsurface mining activity is from literature sources (e.g. 5, 37). Consequently, *Subsidence* rate data carries significant uncertainty and prohibits making more precise predictions of the future trends of delta surface positions.

Results

SRTM data reveal deltas with significant areas (100's to 10,000's km^2) of vulnerable lowlands at elevation <2 m of mean sea level (Table 1), and thus susceptible to river floods and inundation from storm surges, especially those deltas subject to tropical storms (Supplementary Figure 11). Many deltas have large areas below mean sea level (Fig. 1) that are protected from ambient coastal inundation via natural barriers (e.g. beach ridges and dunes), engineered structures, or some combination (e.g. Po, Vistula, Nile, and the Yellow/Huanghe). Thirty-three deltas have a combined area of 26,000 km^2 below mean sea level. The Pearl delta, China, and the Mekong delta, Vietnam, both inhabitated by millions of people and exposed to typhoons, seem particularly vulnerable with much of their surface area below mean sea level, and limited coastal barrier protection (Fig. 2). The Irrawaddy delta shows extensive lowland, and it is therefore understandable how a significant coastal surge, such as associated with Cyclone Nargis, could so easily inundate large parts of this delta in 2008 (Fig. 3).

21st Century *Aggradation* rates have substantively decreased (Table 1), or been nearly or completely eliminated (e.g. Chao Phraya, Colorado, Nile, Po, Tone, Vistula, Yangtze, and the Yellow River deltas). For a few deltas, *Aggradation* has changed little over the 20th century, and remains in balance with, or exceeds *Subsidence* or *Relative Sea Level Rise* (Table 1: e.g. Amazon, Congo, Fly, Orinoco). Some deltas have seen their *Aggradation* rate decreased with engineering, but the rate still exceeds *Subsidence* (Table 1: Amur, Brahmani, Danube, Han, Limpopo, and the Mahanadi). This condition offers a level of protection from storm surges. However, even for a delta, such as the Danube, where subsidence is fully compensated by local tectonic uplift (38), the reduction in sediment load led to a decrease in aggradation, coastal erosion and increased inundation from sea surges (39).

Other deltas experience a *Subsidence* rate much greater than even early 20th Century *Aggradation* (Table 1: Chao Phraya, Ganges, Irrawaddy, Mahakam, Mekong, Mississippi, Niger, Nile, Pearl, Po, Sao Francisco, Tigris, and the Yangtze). For these deltas, *Accelerated Compaction* brought on by human activities is an overwhelming reason why the delta is sinking. For other deltas, a reduced *Aggradation* rate is the overwhelming reason why the delta is sinking, e.g. Colorado, Godavari, Indus, Krishna, Magdalena, Parana, Rhone, Tone, and the Vistula. Yet many deltas suffer both from *Accelerated Compaction* and greatly reduced *Aggradation* rates, e.g. Chao Phraya, Colorado, Krishna, Nile, Pearl, Po, Rhone, Sao Francisco, Yangtze and the Yellow (Table 1).

Based on these data, hypothesis (1) is accepted. Many (71%) of the representative deltas are indeed sinking. Hypothesis (2) is modified to allow for the equally important impact of *Accelerated Compaction* on delta sinking, as well as the greatly reduced *Aggradation*, from both a decrease in the incoming sediment load, and from levee control on delta plain flooding. Fifty percent of the sinking deltas are influenced by both components. Hypothesis (3) is also accepted; local human activities are largely responsible for present vulnerability of deltas.

Daily satellite imagery has been collected only for the last decade, too short an interval to confirm the full extent of flooded areas on deltas. However, over the last decade, half of the represented deltas experienced coastal inundation from surges (Table 1), with the Mahanadi, Yellow, Mississippi, Krishna, Tigris, Indus, and Irrawaddy of note. Many deltas experienced floods from rivers overbanking their levees (Table 1), with the Parana, Vistula, Chao Phraya, Ganges, Pearl,

Danube, Krishna, Rhone, Mekong, and the Brahmani of note. Many deltas were partially flooded from intense rainfall and its associated local runoff within the delta (Table 1), with the most susceptible deltas being the Mississippi, Mahanadi, Krishna, Mekong, Brahmani, and the Ganges. In 2007/08 alone, the following deltas had substantial areas flooded: Ganges, Mekong (Fig. 3), Irrawaddy (Fig. 3), Chao Phraya, Brahmani, Mahanadi, Krishna, and Godavari (Supplementary Figures 2-8), with >100,000 lives lost and more than a million habitants temporarily displaced. Satellite imagery further reveals that often the flooding is not contributing much sediment accumulation, both for reasons of upstream reservoir trapping and from in place levees. The imagery thus qualitatively supports the reduced 21st Century *Aggradation* rates in Table 1. Two exceptions are provided in Fig. 3. The Mekong, from river-borne sediment, and the Irrawaddy, from marine-borne sediment, both saw much sediment added to their delta surface.

Another reason why recent *Aggradation* rates are so low is the reduction in the number and mobility of natural distributary channels. Thirteen of the major deltas saw their distributary channel number decrease, some markedly (Table 1), with the Magdalena, Nile, Vistula, Yellow and the Indus showing all ~ 70-80% reductions. The Indus delta provides a classic example of how through the nineteenth century, and earlier (40), river distributary channels migrated across the delta surface (Fig. 4). SRTM topographic data reveal the lobate sediment deposits from the ancient crevasse splay and paleo-river channels (Fig. 4a). Distributary channels were numerous, and successive surveys show channels to have been mobile (Fig. 4b). To better use precious water resources on the Indus floodplain, an elaborate 20th Century irrigation system was put in place (Fig. 4c) that captured much of the water, sediment and nutrients. Today very little water and sediment makes it to the delta plain through its remaining connection to the ocean (1, 41, Table 1). Channels on deltas are often stabilized and provide a perceived sense of safety of riverside towns (5). In the Nile delta, the sediment escaping the upstream Aswan dam, which is already less than 2% of the original sediment load, is almost completely trapped by a dense network of irrigation channels in the delta (42). The remaining five Po distributary channels still trap 16% of the sediment delivered to the delta, but the sedimentation occurs strictly within the distributary channels themselves and not on the surrounding flood plains which are often well below sea level (30). Ironically, delta-wide aggradation rates may have reduced, but local differential relief may result in increased flood risk.

Summary & Conclusions

Humans are fundamentally altering the functioning of deltas at the global scale. Humans have altered deltaic coastlines through coastline occupation and stabilization. But behind these coastal structures the analyzed major deltas show a combined vulnerable area of 96, 000 km^2 near local sea level. This area would increase to ~143,000 km^2 over the 21st Century if global sea level continues to rise rapidly (8) and we consider vulnerable delta lowlands to be <3 m a.s.l. Furthermore, these lowlands are likely to expand from both reduced *Aggradation* and *Accelerated Compaction* due to hydrocarbon and water withdrawal (36, 37). Humans have engineered most of the natural river discharge delivered to the coast across the delta plain, through up-basin sediment capture and flood wave mitigation. They have stabilized many delta distributary channels and reduced their number, thereby altering the sediment pathways to the coast. Human occupation and infrastructure development continues through the development of delta megacities and their expanding footprint. Without budgeting for the major human contribution to delta sinking, more and more of our world's wetlands will be drowned, while the threats to human activities within deltas will continue to grow.

Global-warming induced sea-level rise is adding to this bleak scenario. An additional immediate impact of global-warming will be changes in magnitude and frequency of hurricanes and

cyclones (43,44), and more intense precipitation events (45). While humans have worked to master the everyday behavior of lowland rivers; they are less able to deal with the fury of extreme events that either cause extensive flooding or that can wash ashore ocean water, with surges 3 to 10 m above mean sea level. The management of delta systems faces a number of fundamental challenges, and the different components adding to the extent of vulnerable area must be precisely addressed if deltaic areas are not to substantially decline with disastrous consequences for the environment and delta residents. It remains alarming how often deltas flood, whether from hurricanes or storm fronts, from land or from sea; river and delta flooding already appears to be increasing and will likely increase in the coming century.

References and Notes

1. Syvitski, J.P.M., Saito, Y. Morphodynamics of Deltas under the Influence of Humans. *Global Planet, Change* **57**, 261-282 (2007).

2. Woodroffe, C.D., Nicholls, R.J., Saito, Y., Chen, Z. & Goodbred, S.L. Landscape variability and the response of Asian megadeltas to environmental change in *Global Change and Integrated Coastal Management: the Asia-Pacific Region, Coastal Systems and Continental Margins, Vol. 10*, N. Harvey, Ed., (Springer, NY, 2006), pp. 277-314.

3. Sanchez-Rodriguez, R. *et al*., Introduction to the "Global Environmental Change, Natural Disasters, Vulnerability and their implications for Human Security in Coastal Urban Areas" Issue *IHDP Update* **2**, 4-5 (2007).

4. Nicholls, R.J. *et al*., Coastal systems and low-lying areas. in *Climate Change 2007: Impacts, Adaptation and Vulnerability. Contribution of Working Group II to the Fourth Assessment Report of the Intergovermental Panel on Climate Change*. M.L. Parry, O.F. Canziani, J.P. Palutikof, P. van der Linden, C.E. Hanson, Eds. (Cambridge University Press, UK, 2007) pp.315-357.

5. Syvitski, J.P.M. Deltas at risk. *Sustainability Science* **3,** 23-32 (2008).

6. Nicholls, R.J. Coastal flooding and wetland loss in the 21st century: changes under the SRES climate and socio-economic scenarios. *Global Environ. Change* **14**, 69-86 (2004).

7. Bindoff, N.L. et al. Observations: Oceanic Climate Change and Sea Level. in *Climate Change 2007: The Physical Science Basis. Contribution of Working Group I to the Fourth Assessment Report of the Intergovernmental Panel on Climate Change*, S. Solomon, et al. Eds. (Cambridge University Press, New York, 2007).

8. Church, J.A., White, N.J. A 20th century acceleration in global sea-level rise. *Geophysical Research Letters* **33**, L01602. doi:10.1029/2005GL024826 (2006).

9. Milne, G.A., Mitrovica, J.X. Searching for eustasy in deglacial sea-level histories. *Quaternary Science Reviews*. doi:10.1016/j.quascirev.2008.08.018 (2008).

10. Jouet, G, Hutton, E.W.H., Syvitski, J.P.M., Rabineau, M. & Berné, S. Modeling the isostatic effects of sealevel fluctuations on the Gulf of Lions *Computers & Geosciences* **34**, 1338-1357 (2008).

11. Blum, M.D. Tomkin, J.H., Purcell, A. Lancaster, R.R. Ups and downs of the Mississippi Delta. *Geology* **36**, 675-678 (2008).

12. Ivins, E.R., Dokka, R.K. & Blom, R.G. Post-glacial sediment load and subsidence, in coastal Louisiana. *Geophys. Res. Lett.* **34** doi:10.1029/2007GL030003 (2007).

13. Dokka, R.K., Sella, G.F. & Dixon, D.H. Tectonic control of subsidence and southward displacement of southeast Louisiana with respect to stable North America. *Geophys. Res. Lett.* **33** doi:10.1029/2006GL027250 (2006).

14. Hutton E.W.H. & Syvitski, J.P.M. SedFlux2.0: New advances in the seafloor evolution and stratigraphic modular modeling system. *Computers & Geosciences* **34**, 1319–1337 (2008).

15. Supplementary materials and methods are available online.

16. Meckel, T. A., Ten Brink, U. S. & Williams, S. J. Sediment compaction rates and subsidence in deltaic plains: numerical constraints and stratigraphic influences. *Basin Research* **19**, 19-31 (2007).

17. Törnqvist, T. E. *et al*. Mississippi Delta subsidence primarily caused by compaction of Holocene strata. *Nature Geoscience* **1**, 173-176 (2008).

18. Han M, Hou J, Wu L. Potential impacts of sea level rise on China's coastal environment and cities: a national assessment. *J. Coastal Res.* **14**, 79-90 (1995).

19. Dixon, T.H. Earth Scientists and Public Policy: Have we failed New Orleans? *Eos Trans. AGU* **89**, 96 (2008)

20. Stephens, J.C., Allen, L.H., Chen, E. Organic soil subsidence. in *Man-Induced Land Subsidence,* T.L. Holzer Ed., Rev. Eng. Geol. Ser. **VI**, 107-122 (1984).

21. Morton, R.A., Bernier. J.C., Barras, J.A. & Ferina, N.F. *Rapid subsidence and historical wetland loss in the Mississippi delta plain: likely causes and future implications*. USGS Open File Report **2005-1216**, 124 pp. (2005).

22. Abam, T.K.S. Regional hydrological research perspective in the Niger Delta *Hydrological Sciences* **46**, 13-25 (2001).

23. Saito Y., Chaimanee N., Jarupongsakul, T., & Syvitski, J.P.M. Shrinking megadeltas in Asia: Sea-level rise and sediment reduction impacts from case study of the Chao Phraya delta. *Inprint Newsletter of the IGBP/IHDP Land Ocean Interaction in the Coastal Zone* **2007/2**, 3-9 (2007).

24. Caputo, M., Pieri, L., Unghendoli, M. Geometric investigation of the subsidence in the Po Delta. *Boll. Geofis. Teor. Appl.* **14**, 187-207 (1970).

25. Bondesan, M., Simeoni, U. Dinamica e analisi morfologica statistica dei litorali del delta del Po e alle foci dell'Adige e del Brenta. *Mem. Sci. Geol.* **36**, 1-48 (1983).

26. Simeoni, U., Fontolan, G., Tessari, U. & Corbau, C. Domains of spit evolution in the Goro area, Po Delta, Italy. *Geomorphology* **86**, 332-348 (2007).

27. Day, J.W., Jr. *et al.* Restoration of the Mississippi Delta: Lessons from Hurricanes Katrina and Rita. *Science* **315**, 1679-1684 (2007).

28. Turner, R.E., Swenson, E.M. Milan, C.S. & Lee, J.M. Hurricane signals in salt marsh sediments: Inorganic sources and soil volume. *Limnol. Oceanogr.* **52**, 1231-1238 (2007).

29. Turner, R.E. Baustian, J.J. Swenson, E.M. & Spicer, J.S. Wetland Sedimentation from Hurricanes Katrina and Rita. *Science* **314**, 449-452 (2006).

30. Syvitski, J.P.M., Kettner, A.J., Correggiari, A. & Nelson, B.W. Distributary channels and their impact on sediment dispersal. *Marine Geology* **222-223**, 75-94 (2005).

31. Yu, L. The Huanghe (Yellow) River: Recent changes and its countermeasures. *Cont. Shelf Res.* **26**, 2281-2298 (2006).

32. J.W. Day, Jr., *et al*. Pattern and process of land loss in the Mississippi Delta: A Spatial and Temporal Analysis of Wetland habitat change. *Estuaries* **23**, 425-438 (2000).

33. Schumann, G. *et al*., Comparison of remotely sensed water stages from LiDAR, topographic contours and SRTM. *ISPRS J. Photogrammetry & Remote Sensing* **63**, 283-296 (2008).

34. Milliman, J.D. & Syvitski, J.P.M. Geomorphic/tectonic control of sediment discharge to the ocean: The importance of small mountainous rivers. *J. Geology* **100**, 525-544 (1992).

35. Syvitski, J.P.M. & Milliman, J.D. Geology, geography and humans battle for dominance over the delivery of sediment to the coastal ocean. *Geology* **115**, 1-19 (2007).

36. Roldolfo, K.S. & Siringan, F.P. Global sea-level rise is recognised, but flooding from anthropogenic land subsidence is ignored around northern Manila Bay, Philippines. *Disasters* **30**, 118-139 (2006).

37. Ericson, J.P., Vörösmarty, C.J., Dingman, S.L., Ward, L.G. & Meybeck, M. Effective sea-level rise and deltas: causes of change and human dimension implications. *Global Planet. Change* **50**, 63-82 (2006).

38. Giosan, L. *et al*., Young Danube delta documents stable Black Sea level since the middle Holocene: Morphodynamic, paleogeographic, and archaeological implications. *Geology* **34**, 757-760 (2006).

39. Giosan, L., Bokuniewicz, H.J., Panin, N. & Postolache, I. Longshore sediment transport pattern along the Romanian Danube delta coast*J. Coastal Res*. **15**, 859-871 (1999).

40. Holmes, D.A. The Recent History of the Indus. *The Geog. J*. **134**, 367-382 (1968).

41. Giosan, L. *et al*. Recent morphodynamics of the Indus delta shore and shelf. *Cont. Shelf Res*. **26**, 1668-1684 (2006).

42. Stanley, J.D. & Warne, A.G. Nile delta in its destructive phase, *J. Coastal Res.* **14**, 794-825 (1998).

43. Goldenberg, S.B. *et al*. The recent increase in Atlantic hurricane activity: causes and implications. *Science* **293**. 474-479 (2001).

44. Holland, G., Webster, P. Heightened tropical cyclone activity in the North Atlantic: natural variability or climate trend? Phil. *Trans. R. Soc. A* doi:10.1098/rsta.2007.2083 (2007).

45. Lambert, F.H. Stine, A.R. Krakauer, N.Y. & Chiang, J.C.H. How much will precipitation increase with global warming. EOS, Transactions of AGU, **89**, 193-194 (2008).

Acknowledgements:
We thank the following organizations for their research funding: National Science Foundation (Cooperative Agreement 0621695), NASA (NNXOTAF2SG/P207124; NNXOTAF28G/P207124), and the Office of Naval Research (N00014-04-1-0235). Many scientists have contributed to this effort, including Chris Paola (NCED), Scott Peckham (CSDMS), Won-Suk Kim (U. Illinois U-C), Joep Storms (Delft U. Tech), and Ilan Kelman (Norway).

Table 1. Representative deltas analyzed using MODIS imagery, SRTM data, and ancillary data (see Methodology section and 15 for details). Commentary in the storm surge column is as follows: LP= little potential; MP = moderate potential; SP = significant potential). Net Subsidence (or Relative Sea Level Rise) rates are time variable, and provided ranges cover different times and areas of a delta, where known; question marks are for unknown estimates.

Delta	No. Maps	Est. Area km^2 <2m ASL	Recent Area km^2 Storm Surge	Recent Area km^2 River Flood	Recent Area km^2 In situ Flooding	% Sediment Reduction	Floodplain or Delta Flow Diversion	% Distributary Channel Reduction	Subsurface Water, Oil & Gas Mining	Early 20th C Aggradation Rate mm/y	21st Century Aggradation Rate mm/y	Subsidence mm/y
Amazon, Brazil	6	1960*	0; LP	0	9340	0	No	0	0	0.4	0.4	?
Amur, Russia	-	1250	0; LP	0	0	0	No	0	0	2	1	0.5-2
Brahmani, India	6	640	1100	3380	1580	50	Yes	0	Major	2	1	0
Chao Phraya, Thai.	2	1780	800	4000	1600	85	Yes	30	Major	0.2	0	50-150
Colorado, Mexico	3	700	0; MP	0	0	100	Yes	0	Major	34	0	2-4
Congo¶ DRC	-	460	0; LP	0	0	20	No	0	0	0.2	0.2	0?
Danube, Romania	4	3670	1050	2100	840	63	Yes	0	Minor	3	1	≈0
Fly, PNG	-	70*	0; MP	140	280	0	No	0	0	5	5	0.5
Ganges¶, Bangl.	9	6170*	10500	52800	42300	30	Yes	37	Major	3	2	18
Godavari, India	6	170	660	220	1100	40	Yes	0	Major	7	2	≈4
Han, Korea	-	70	60	60	0	27	No	0	0	3	2	0
Indus, Pakistan	12	4750	3390	680	1700	80	Yes	80	Minor	8	1	1.3
Irrawaddy, Myan.	2	1100	15000	7600	6100	30	No	20	Minor	2	1.4	6
Krishna, India	6	250	840	1160	740	94	Yes	0	Major	7	0.4	≈4
Limpopo, Moz.	-	150	120	200	0	30	No	0	0	7	5	0
Magdalena, Col.	14	790	1120	750	750	0	Yes	70	0	6	3	6.6
Mahakam, Borneo	-	300	0; LP	0	370	0	No	?	0	0.2	0.2	0.5
Mahanadi, India	6	150	1480	2060	1770	74	Yes	40	Moderate	2	0.3	0
Mekong, Vietnam	1	20900	9800	36750	17100	12	No	0	Minor	0.5	0.4	>5
Mississippi, USA	15	7140	13500	0	11600	48	Yes	?	Major	2	0.3	5-25
Niger, Nigeria	9	350*	1700	2570	3400	50	No	30	Major	0.6	0.3	7.5
Nile, Egypt	15	9440	0; LP	0	0	98	Yes	75	Major	1.3	0	5
Orinoco, Venez.	10	1800*	0; MP	3560	3600	0	No	0	Unknown	1.3	1.3	0.8-3
Parana, Argentina	6	3600	0; LP	5190	2600	60	No	?	Unknown	2	0.5	3
Pearl¶, China	4	3720	1040	2600	520	67	Yes	0	Moderate	3	0.5	7.5
Po, Italy	20	630	0; LP	0	320	50	No	40	Major	3	0	4-60
Rhone, France	11	1140	0; LP	920	0	30	No	40	Minor	7	1	2-6
Sao Francisco, Bra.	-	80	0; LP	0	0	70	Yes	0	Minor	2	0.2	10
Tigris¶, Iraq	7	9700	1730	770	960	50	Yes	38	Major	4	2	5
Tone¶, Japan	-	410	220	0	160	30	Yes	§	Major	4	0	>10
Vistula, Poland	4	1490	0; LP	200	0	20	Yes	75	Unknown	1.1	0	0.3
Yangtze¶, China	8	7080	6700	3330	6670	70	Yes	0	Major	1.1	0	10
Yellow¶, China	11	3420	1430	0	0	90	Yes	80	Major	49	0	8

*Significant canopy cover renders these SRTM elevation estimates as conservative values

¶ Alternate names: Congo & Zaire; Ganges & Ganges-Brahmaputra; Pearl & Zhujiang; Tigris & Tigris-Euphrates & Shatt al Arab; Tone & Edo; Yangtze & Changjiang; Yellow & Huanghe

§ The Tone R. has long had its flow path engineered, having once flowed into Tokyo Bay; the number of distributary channels has increased with engineering works.

Color key $20^{th}A \approx 21^{st}A > S$ $20^{th}A > 21^{st}A > S$ $20^{th}A >> 21^{st}A << S$ $20^{th}A >> 21^{st}A < S$ $20^{th}A > 21^{st}A << S$

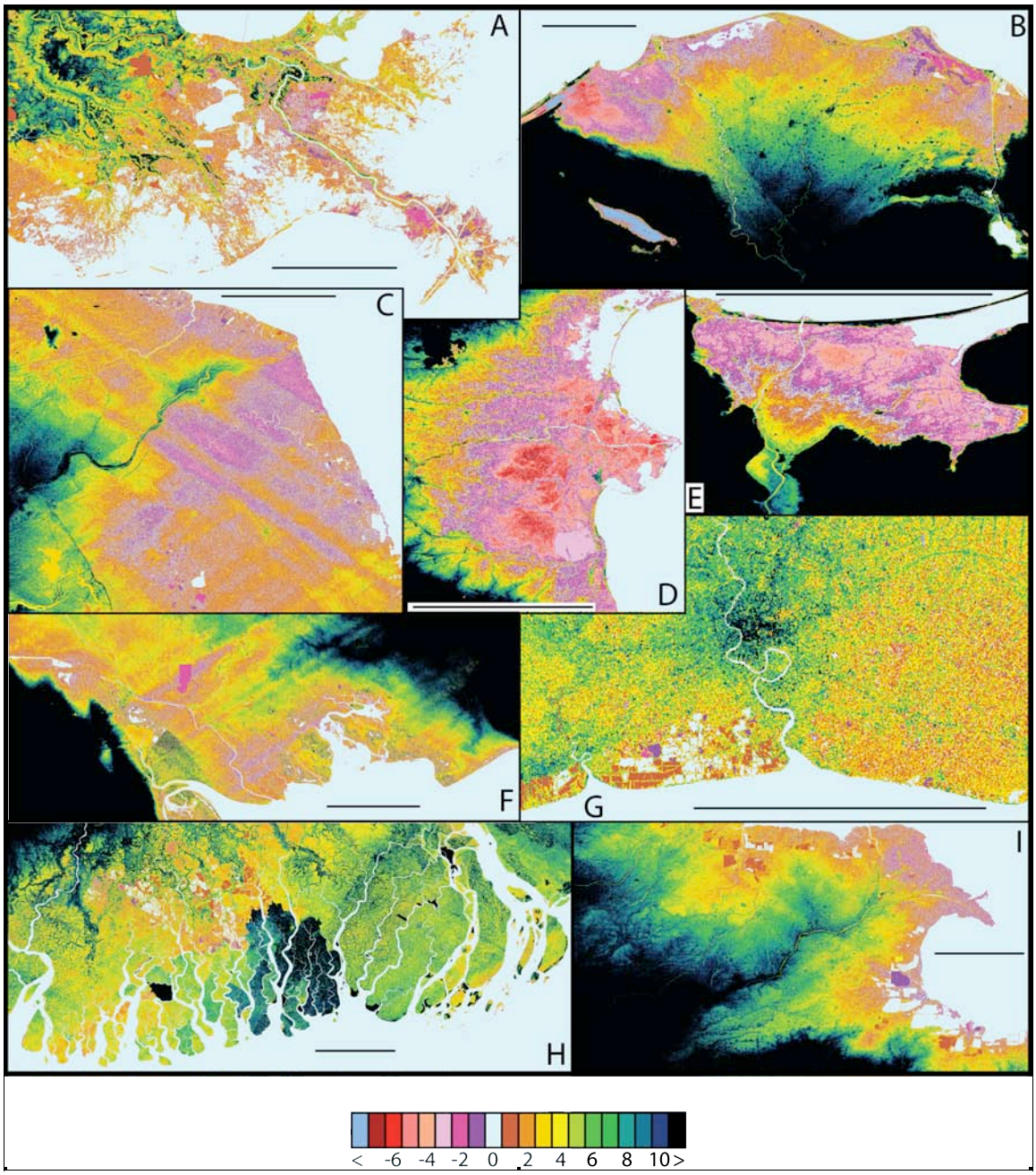

Figure 1: Nine representative deltas, displayed with Space Shuttle Radar (SRTM) altimetry, binned at 1 m vertical intervals, starting at sea level (light blue), then 1 color per 1 m interval, with colors cycled every 10 m, to a height of 100 m, then black. Topography below mean sea level is in shades of pink. A) Mississippi, USA, B) Nile, Egypt, C) Old abandoned Yellow (Huanghe) delta, China, D) Po, Italy E) Vistula, Poland, F) Shatt al Arab (Tigris-Euphrates), Iraq, G) Chao Phraya, Thailand, H) Ganges-Brahmaputra, Bangladesh, and I) Modern (since 1855) Yellow, China. Many areas are <2 m above sea level (brown, yellow, pink). Scale bar on each image represents 50km.

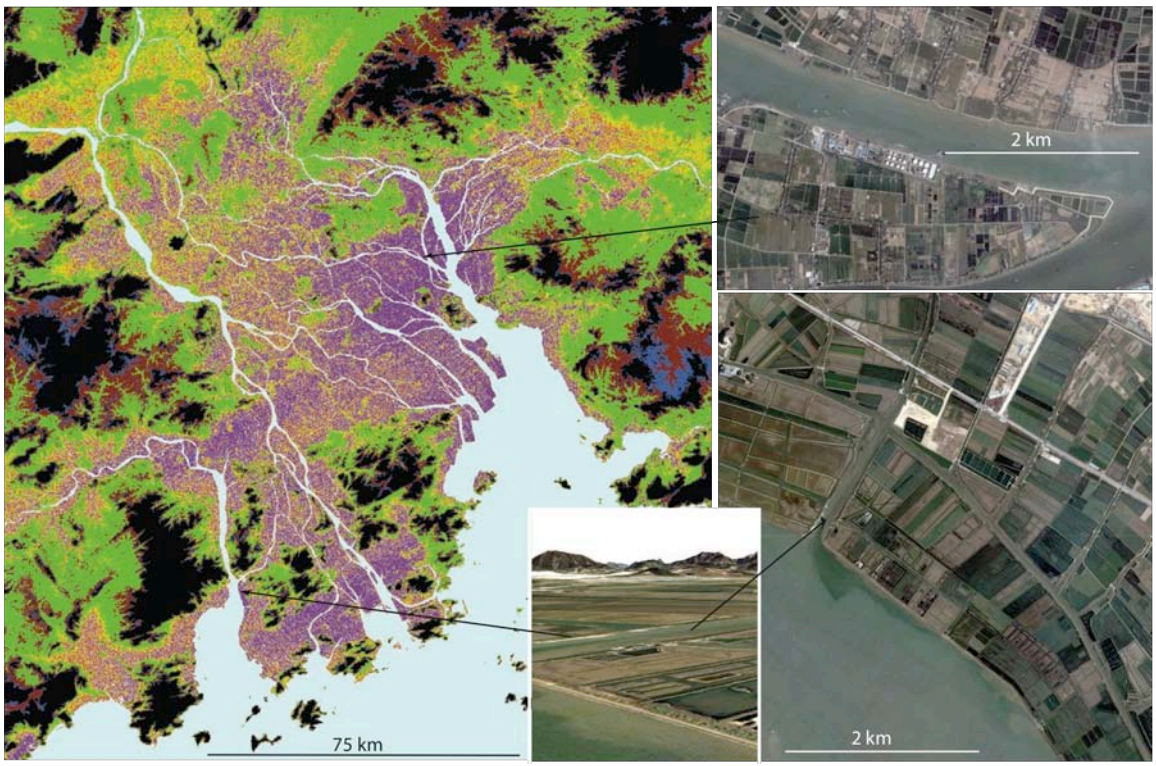

Figure 2: The Pearl delta, China, displayed with Space Shuttle Radar (SRTM) altimetry, binned as follows: purple <0m, light blue 0m, brown 0-1m, light brown 1-2m, dark yellow 2-3m, light green 3-4m, yellow 4-5m, dark green 5-35m, dark brown 35-65m, dark blue 65-95m, and black >95m. Delta portions below sea level are protected from storm surges by coastal and channel barriers as seen (B, C and D) in Digital Globe images served on Google Earth.

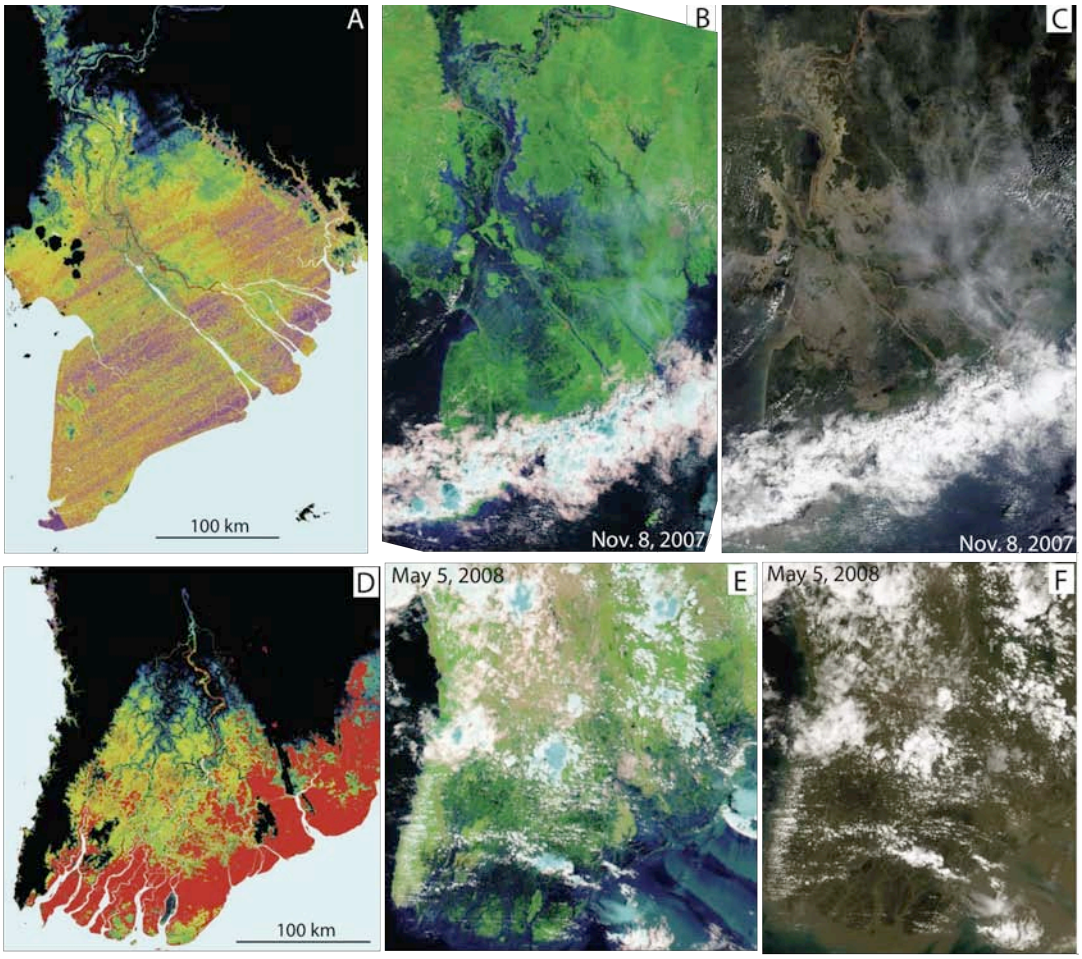

Figure 3: A) Mekong Delta, Vietnam, displayed with SRTM altimetry, binned at 1 m vertical intervals, starting at sea level (light blue), then 1 color per 1 m interval, to a height of 10 m, then black. Topography below mean sea level is in shades of pink. B) MODIS near infrared image (Nov. 8, 2007), showing flooding of the upper Mekong Delta. C) MODIS true color imagery (Nov. 8, 2007) showing sediment laden floodwaters on the upper Mekong Delta. D) Flood waters shown in red, superimposed on SRTM altimetry. While delta has little area below mean sea level, the coastal surge from Cyclone Nargis was sufficient to drown a significant portion of the lower Irrawaddy delta. E) MODIS near infrared image (May 5, 2008), showing the flooding of the lower Irrawaddy delta caused by Cyclone Nargis. F) MODIS true color imagery (May 5, 2008), showing the sediment laden coastal waters.

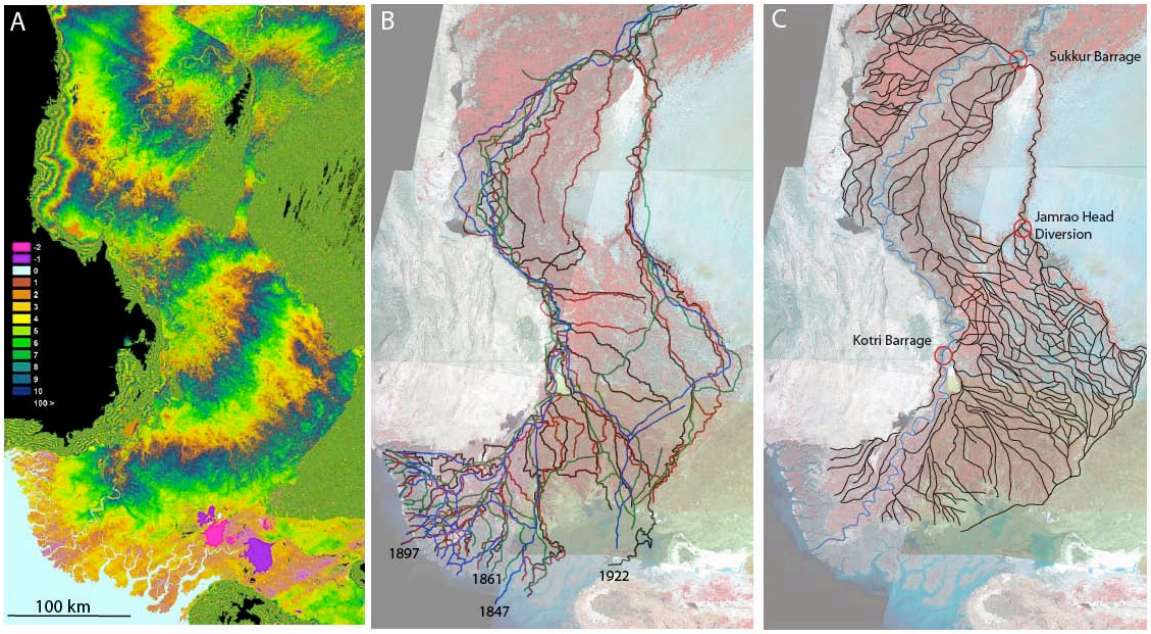

Figure 4: A) The Indus floodplain and Delta (Pakistan) displayed with SRTM altimetry, binned at 1 m vertical intervals, starting at sea level (light blue), then 1 color per 1 m interval, with colors cycled every 10 m, to a height of 100 m, then black. Topography below mean sea level is in shades of pink. B) 1) Historical location of distributary channels (cartographer, color, year and registration error): Weiland, blue, 1847, ±3.8 km; Johnston, green, 1861, ±3.8 km; Rand McNally, red, 1897, ±3.7 km; and Bartholomew, black, 1922, ±3.1 km. C) Irrigation channel system with main water distribution stations.